HHS Public Access

Author manuscript

Soft Matter. Author manuscript; available in PMC 2018 February 08.

Published in final edited form as:

Soft Matter. 2017 February 08; 13(6): 1223–1234. doi:10.1039/c6sm02756c.

Flory theory of randomly branched polymers

Ralf Everaers[a], **Alexander Y. Grosberg**[b], **Michael Rubinstein**[c], and **Angelo Rosa**[d]

[a]Univ Lyon, ENS de Lyon, Univ Claude Bernard Lyon 1, CNRS, Laboratoire de Physique and Centre Blaise Pascal, F-69342 Lyon, France

[b]Department of Physics and Center for Soft Matter Research, New York University, 726 Broadway, New York, NY 10003, USA

[c]Department of Chemistry, University of North Carolina, Chapel Hill, NC 27599, USA

[d]SISSA - Scuola Internazionale Superiore di Studi Avanzati, Via Bonomea 265, 34136 Trieste, Italy

Abstract

Randomly branched polymer chains (or trees) are a classical subject of polymer physics with connections to the theory of magnetic systems, percolation and critical phenomena. More recently, the model has been reconsidered for RNA, supercoiled DNA and the crumpling of topologically-constrained polymers. While solvable in the ideal case, little is known exactly about randomly branched polymers with volume interactions. Flory theory provides a simple, unifying description for a wide range of branched systems, including isolated trees in good and θ-solvent, and tree melts. In particular, the approach provides a common framework for the description of randomly branched polymers with quenched connectivity and for randomly branch*ing* polymers with annealed connectivity. Here we review the Flory theory for interacting trees in the asymptotic limit of very large polymerization degree for good solvent, θ-solutions and melts, and report its predictions for annealed connectivity in θ-solvents. We compare the predictions of Flory theory for randomly branched polymers to a wide range of available analytical and numerical results and conclude that they are qualitatively excellent and quantitatively good in most cases.

Graphical abstract

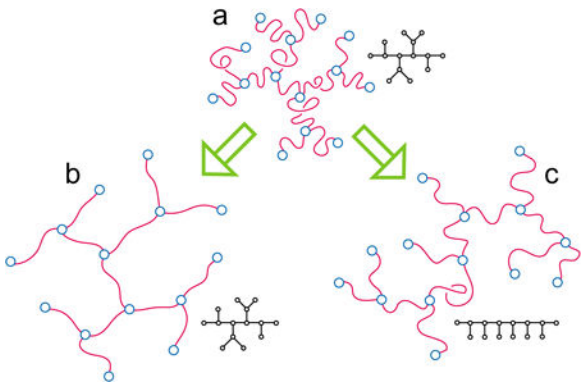

Correspondence to: Angelo Rosa.

Different swelling modes for branched polymers (a) with quenched (b) and annealed connectivity (c) are explained by the Flory theory.

1 Introduction

Randomly branched polymers, or trees for brevity, are of interest in a number of scientific fields. Branched polymers can be synthesised by deliberately incorporating monomers with higher functionality into the polymerisation processes as a means of modifying materials properties[1,2]. In industrial applications they represent the norm rather than the exception, since most polymerisation processes for linear chains also introduce a certain amount of branching, a feature that strongly affects the dynamics[3].

In the same way as random walks can be used as models for linear polymers, random trees are models for branched polymers. In this article, we use the term “tree” not only for the model, but also as a convenient short-hand notation for the object.

Theoretical models for trees date back to the early days of polymer physics[4], and have been successfully employed since then in the description of a wide range of phenomena including percolation[5] and gelation[1]. More recently, these models have been reconsidered in the context of biological molecules. In fact, the large RNA's of some viruses (Fig. 1a) behave in many ways like branched polymers owing to the presence of (small) multi-loops in the secondary structure which effectively act as branching points[6–8]. Similarly, supercoiled circular DNA inside the bacterial nucleoid folds into plectonemic structures[9,10] which can branch on larger scales (Fig. 1b). In Statistical Mechanics, the closely related subject of lattice animals[11–13] has deep connections with magnetic spin systems and has been studied by field theoretic methods[14–17]. Our own (renewed) interest in these systems[18–20] is due to the analogy between their behavior and the crumpling of topologically constrained ring polymers[21–25] (Fig. 1c) and, ultimately, chromosomes[26–30].

While there is a number of exact results for ideal, non-interacting trees[4,32,33], even the simplest theory of the systems described above may not ignore the excluded volume interactions between the constituents of the trees. The treatment of these interactions is notoriously difficult even for linear polymers[34]. In practice[1,35], descriptions are often limited to the level of scaling arguments[36] and Flory theory[37]. In the case of branched chains, there is a single exactly known exponent for isolated three-dimensional self-avoiding trees[14], highlighting the need for approximate treatments. Here we focus on Flory theories[11,18,33,38], which provide a unifying description of the rich behaviour of a wide range of tree systems. Our aim is twofold: firstly, we provide a pedagogical, comprehensive review of the theory; secondly, we compare the predictions to available theoretical[14,16,39–49] and computational[50–63] results to gauge the reliability of the approach. We find that predictions of Flory theory are qualitatively excellent. The predicted values of the Flory exponent ν describing the scaling of polymer size with its mass are quantitatively accurate and agree with best numerical estimates in many cases.

The work is structured as follows. In Section 2 we introduce the model and discuss the theoretical difficulties arising from branching. Furthermore we briefly review the

observables and exponents, which serve to characterize the connectivity and spatial configuration of randomly branched polymers. In particular, we carefully distinguish between randomly branch*ed* polymers with quenched connectivity (in short, *quenched trees*), whose connectivity remains "frozen" after their initial preparation, and randomly branch*ing* polymers with annealed connectivity (in short, *annealed trees*), whose connectivity can adapt to the environmental conditions. Section 3 is devoted to a review of Flory theory. We discuss the underlying ideas and work out the predictions for isolated trees in good and θ-solvent as well as for tree melts. In all cases, we discuss trees with annealed connectivity as well as trees with the quenched connectivity of ideal random trees. In Section 4 we compare the results to available theoretical and numerical estimates of the asymptotic exponents. Finally, in Section 5 we draw the conclusions by also commenting briefly on the theoretical limitations of the Flory theory.

2 Interacting trees

Trees are spatially embedded graphs, which are free of closed paths or loops. Ideal random trees are composed of $N+1$ nodes or monomers, which are randomly connected by N bonds. We treat these bonds as having a uniform (Kuhn) length, l_K. In the absence of branching, ideal trees reduce to freely jointed chains of contour length, $L = l_K N$, and mean-square end-to-end distance, $\langle(\vec{r}_N - \vec{r}_0)^2\rangle = l_K L$. The subject of this article are *interacting* random trees, i.e. trees whose nodes/monomers interact with each other via short-range excluded volume interactions.

The theory of branched polymers is more difficult than linear ones for at least three reasons. **First**, branched polymers are considerably more compact than their linear counterparts and therefore volume interactions play a more important role. Indeed, for isolated non-interacting randomly branched polymers, the root-mean-square gyration radius scales with polymerization degree N as $R \sim \langle R_g^2 \rangle^{1/2} \sim N^{1/4}$ compared to $N^{1/2}$ for ideal linear polymers[4]. **Second**, to characterise a branched polymer, or an ensemble of randomly branched polymers, one has to describe two aspects – their connectivity (or topology of branching, or internal geometry) as well as their conformations (or embedding in space). The latter, in the simplest case, is commonly characterised through the root mean square gyration radius, $R \sim \langle R_g^2 \rangle^{1/2}$, or root-mean-square *spatial* distance between monomers, just as in the linear polymer case. But the former is peculiar for branched systems only. A useful measure of connectivity is the average value of the *contour* distance between all possible pairs of monomers i, j, $L \sim \langle \ell_{ij} \rangle$, which is equally a measure of the average length of linear paths on the tree. Thus, even the simplest theory of branched polymers has to operate with two *distinct* observables, R and L. And the **third** inherent peculiarity of branched systems is the necessity to distinguish between annealed (randomly branching) and quenched (randomly branched) polymers, or trees[38]. Let us explain this point in more detail.

According to accepted terminology, quenched trees are the ones in which the topology of branches, or simply the value of L, is fixed during synthesis and does not change afterwards. In contrast, the topology of annealed trees, or their L parameter, is not fixed by synthesis, but instead varies in response to external conditions and fluctuates due to thermal motion. Note

that linear chains in this context can be thought of as a trivial limit of quenched tree with $L \sim N$. As one example, chemically synthesized branched polymers have almost always quenched connectivity. RNA can rearrange its secondary structure, therefore, it should be viewed as annealed branching polymer (Fig. 1a). Also ring polymer placed in a lattice of immobile uncrossable obstacles (Fig. 1c) behaves like an annealed branching polymer[21,22].

Considering sufficiently large polymers ($N \gg 1$), we will be interested in this article only in scaling relations. We first define the usual scaling exponent ν, which characterizes the dependence of polymer size, R, on the degree of polymerization N:

$$R \sim N^{\nu}; \quad (1)$$

$1/\nu = d_f$ is the corresponding fractal dimension. Next we define the index ρ, which characterizes the branching topology and relates the parameter L to the degree of polymerization N:

$$L \sim N^{\rho}. \quad (2)$$

Finally, we define the scaling exponent ν_{path} relating chain size R and characteristic chemical length L:

$$R \sim L^{\nu_{\text{path}}}; \quad (3)$$

this index tells us how a typical linear chemical path in the tree, viewed as a linear polymer, is embedded in space; $1/\nu_{\text{path}} = d_f^{\text{path}}$ is the fractal dimension of a typical single chemical path of the tree in space.

It is immediately clear from the definitions that in general,

$$\nu_{\text{path}} = \nu/\rho. \quad (4)$$

Furthermore, since chemical paths on a tree cannot include more steps than monomers present, we have $\rho < 1$. Similarly, the spatial extension of trees and path cannot exceed their total contour length, so that $\nu < 1$ and $\nu_{\text{path}} < 1$.

There are not very many cases where critical exponents ν and ρ are known exactly. For isolated, non-interacting trees $\nu = 1/4$ (compared to $\nu = 1/2$ for linear chains) while $\rho = 1/2$, and this is true for both quenched and annealed cases[4]. For isolated, self-avoiding lattice trees with annealed connectivity in $d = 3$, the analogy to lattice animals[14] allows to obtain the exact result $\nu = 1/2$ but it gives no prediction for ρ.

3 Flory theory

Flory theories [37,64] are formulated in terms of a balance between elastic and interaction contributions to the free energy

$$\mathscr{F}=\mathscr{F}_{el}+\mathscr{F}_{\text{inter}}. \quad (5)$$

Although physically appealing, this representation of the free energy is itself an approximation; in reality, these terms in the free energy are not independent from one another. As a result, although minimization of Flory free energy (5) yields very good approximations for the gyration radius for linear polymers, and, as we will see also for branched ones, the value of the free energy corresponding to this minimum itself is severely in error. Therefore, we can not overemphasize the fact that one must exercise great caution to use Flory theory for the right purpose. Elucidating corresponding applicability limits for various *randomly* branched systems is one of the goals of this article. Although not explicitly discussed here, it is worth mentioning that Flory theories have been equally formulated for *regularly* (opposed to randomly) branched polymers such as: star polymers[65,66], dendrimers[67,68] and dendronized polymers and forests[68].

Returning to Eq. (5), the interaction free energy, $\mathscr{F}_{inter}$, is assumed to be independent of the connectivity and depends only on the overall density of the monomer cloud, i.e., on R. In contrast, the elastic energy of trees, $\mathscr{F}_{el}$, is very sensitive to the monomeric connectivity. It depends not only on the spatial distance between nodes, R, but also on their typical contour distance, L. We, therefore, begin with the discussion of this elastic free energy.

3.1 Entropic elasticity of trees

3.1.1 Quenched trees—For quenched branched polymers the parameter L is controlled by the synthesis condition and does not change in reaction to external forces or intermolecular interactions. For a given connectivity, to increase the spatial distance between any two nodes, the linear paths connecting them need to elongate/straighten in space, as sketched in Fig. 2. Qualitatively, as a consequence, the smaller L, the more energy is required to reach a given average spatial distance, R. Quantitatively, the corresponding elastic free energy is[69]:

$$\frac{\mathscr{F}_{el}}{k_B T}\sim\frac{R^2}{I_K L}. \quad (6)$$

This expression is highly non-trivial, as it looks like stretching free energy of a single linear chain of L/l_K segments, each segment corresponding to a Kuhn statistical unit[70] of linear size = l_K; in other words, it looks like it accounts for the deformation of only one chemical backbone out of many branches present in the polymer, while in reality all branches swell in fractal manner. A rigorous proof of Eq. (6) is given in[71], where it is shown that, up to

logarithmic corrections, $\frac{\mathscr{F}_{el}}{k_B T} \sim \frac{R^2}{l_K^2 \mu}$ with $\mu \sim L/l_K$ being the largest eigenvalue of the Kramers matrix† associated to the quenched branched polymer.

3.1.2 Annealed trees—In contrast to quenched polymers, annealed branching polymers swell or respond to stretching in two different ways, sketched in Fig. 2 (right): they extend their linear sections and reconfigure their branching topology, described by two terms for the elastic free energy:

$$\frac{\mathscr{F}_{el}}{k_B T} \sim \frac{R^2}{l_K L} + \frac{L^2}{N l_K^2}, \quad (7)$$

The first term is the same as in the quenched polymer case, and it describes the same mode of swelling, while the major novelty is the second term, which describes entropy of reconfiguring the tree topology.

This term can be derived formally from the partition function of all trees of N bonds and with the L bonds between two arbitrary fixed ends. The derivation employs the diagrammatic recursive method presented in Refs. [32,33] with the simplifying assumption[38] that only ends and branchings are allowed (no bifunctional units or linear parts). Suggestively, an intuitive way to understand the second term in Eq. (7) is to imagine tree-like graphs as drawn on an abstract Cayley tree. Then L/l_K is just a "gyration radius" in that space, and $(L/l_K)^2/N$ is just the usual elastic free energy of a Gaussian polymer.

Since L for annealed polymer is a fluctuating quantity, free energy Eq. (7) reduces after optimization of L at fixed R to obtain

$$L \sim \left(R^2 l_K N\right)^{1/3} \quad (8)$$

and

†The method of the Kramers matrix[1,7,71,72] allows for a systematic treatment of the elasticity of a quenched branched polymer. The Kramers matrix G is an $N \times N$ matrix, every element of it G_{km} corresponds to two bonds in the graph, k and m. These two bonds delineate one portion of the tree with $K(k)$ monomers on one side of bond k, another portion with $M(m)$ monomers on the other side of bond m, with the rest of the monomers between two bonds, and then $G_{km} = \pm K(k)M(m)/N^2$, where the sign+ or − is chosen according to a simple rule. The trace of the Kramers matrix gives the mean square gyration radius of the tree without volume interactions (Kramers theorem, see[1]). And if the tree swells (or is being pulled) much in excess of this average, than the corresponding elastic free energy can be expressed in terms of the largest eigenvalue of the Kramers matrix, μ: $\frac{\mathscr{F}_{el}}{k_B T} \simeq \frac{3R^2}{2l_K^2 \mu} - \frac{3}{2}\ln\left(\frac{R}{l_K}\right)^2 + \frac{3}{2}\ln\mu$; in this form, the expression is amenable to numerical implementation for RNA[7]. But as far as scaling is concerned, a separate argument is required to establish the connection between μ and L, and it shows $L/l_K \sim \mu$, up to logarithmic corrections [71].

$$\frac{\mathcal{F}_{el}}{k_B T} \sim \left(\frac{R}{l_K N^{1/4}} \right)^{4/3}. \quad (9)$$

This result is consistent with the fact that $R \sim l_K N^{1/4}$ (see[4,32,33]) for ideal, non-interacting trees‡.

3.2 Relation between exponents

The fact that the interaction free energy in Flory approximation is independent of branching, *i.e.* it does not depend on L, yields an interesting testable prediction. To understand it, let us imagine for a moment, say, three annealed trees with the same N and l_K, but placed in different environments: for instance, one tree may be placed alone in a solvent of a certain quality, another tree is surrounded by other trees in a melt or in a concentrated solution, and the third tree is subjected to some external forcing – such that all three happen to have the same overall size R. Then we expect all of them to have also the same value of L. To make this quantitative, let us return to the minimization of free energy (7) with respect to L, Eq. (8). If we write $R \sim N^{\nu}$ and $L \sim N^{\rho}$, then we arrive at the following general relation between indices ν and ρ:

$$\rho = \frac{1+2\nu}{3}; \quad (10)$$

in the light of Eq. (4), this is also equivalent to

$$\nu_{\mathrm{path}} = \frac{3\nu}{1+2\nu}. \quad (11)$$

Eqs. (10) and (11) are plotted in Fig. 4 as the red and green line, respectively. It is worth repeating that these relations follow from the assumed independence of interaction energy from the branching parameter L. To illustrate these relations, let us see how they work in various simple cases. If a system is fully extended, which means $\nu = 1$, then it is predicted not to branch, $\rho = 1$, and to have a fully stretched stem, $\nu_{\mathrm{path}} = 1$. For the radius of ideal randomly branched polymers, $\nu^{\mathrm{ideal}} = 1/4$, one recovers the Zimm-Stockmayer result $\rho^{\mathrm{ideal}} = 1/2$[4] and Gaussian path statistics, $\nu_{\mathrm{path}}^{\mathrm{ideal}} = 1/2$.

‡One may be puzzled by the fact that free energy (9) is minimal at $R = 0$. One way to think about it is to realize that typical fluctuation corresponds to $\mathcal{F}_{el} \sim k_B T$. A better way is to remember that at very small R a more accurate expression must be used for $\mathcal{F}_{el}$, it can be approximated as $\frac{\mathcal{F}_{el}}{k_B T} \sim \left(\frac{R}{l_K N^{1/4}} \right)^{4/3} + \left(\frac{l_K N^{1/4}}{R} \right)^{4}$, it is minimal at the expected finite R. The additional term, which blows up at very small R, is never important in real physics, because even a minimal excluded volume will drive branched polymer to larger R. But if one wants to treat purely mathematical problem of ideal trees without any excluded volume, than extra term of free energy arises from low probability (high entropy cost) of placing all monomers in a small volume.

Relations (10)-(11) suggest a peculiar way to view the problem, by considering index ν as an independent variable. This way, we look in parallel to physically different systems and even having different space dimensions, but as long as they have the same ν – they should have ρ and ν_{path} given by equations (10)-(11) – as long as Flory theory assumption of $\mathscr{F}_{inter}$ being independent of branching is correct. From that point of view, it is easy to establish that $\nu_{\text{path}} - \nu_{\text{path}}^{\text{ideal}} = \frac{4\nu - 1}{2(1+2\nu)} > \frac{4\nu - 1}{6} = \rho - \rho^{\text{ideal}}$ at any $\nu < 1$, where $\nu_{\text{path}}^{\text{ideal}} = 1/2$ and $\rho^{\text{ideal}} = 1/2$; we can interpret this saying that path stretching contributes more to the overall swelling than rearrangement of branches, as long as the trees are not fully stretched, i.e., as long as $\nu < 1$ (note that at $\nu = 1$ automatically also $\rho = \nu_{\text{path}} = 1$). Similarly, we can consider the case when ν is close to $\nu^{\text{ideal}} = 1/4$, which corresponds to weakly swollen trees; in that case, Eqs. (10) and (11) imply that $\nu_{\text{path}} - \nu_{\text{path}}^{\text{ideal}} \approx 2(\rho - \rho^{\text{ideal}}) = 4(\nu - \nu^{\text{ideal}})/3$.

3.3 Flory theory for trees with volume interactions

In his original formulation for linear chains in good solvent[37], Flory considered the two-body repulsion between segments, described by the second virial approximation. To cover also higher order collisions, θ-conditions, and melts, we use the more general form

$$\frac{\mathscr{F}_{\text{inter}}^{(p,x)}}{k_B T} \sim \frac{1}{N^x} \nu_p \frac{N^p}{R^{(p-1)d}} \quad (12)$$

for the pth moment of the virial expansion. Screening in a melt is accounted for by setting $x \equiv 1$[11], while for isolated chains in dilute solution $x \equiv 0$. Eq. (12) reduces to the standard form, $\frac{\mathscr{F}_{\text{inter}}}{k_B T} = \nu_2 \frac{N^2}{R^d}$, for $p = 2$ and $x = 0$. As repeatedly stated above, interaction free energy in Flory approximation does not depend on L.

Next we minimize the total Flory free energy with respect to R.

3.3.1 Quenched branched polymer—For branched polymers with quenched connectivity, the variational free energy per chain includes the elastic contribution, Eq. (6), and the interaction term, Eq. (12). Substituting $L \sim N^p$, and minimizing the sum with respect to R we find

$$\nu = \frac{p + \rho - x}{(p-1)d + 2} \quad (13a)$$

$$\nu_{\text{path}} = \frac{1}{\rho} \frac{p + \rho - x}{(p-1)d + 2} \quad (13b)$$

where Eq. (13b) follows directly via Eq. (4). Note that ρ here is controlled by how the macromolecule was synthesized.

Every chemical path in the tree cannot be stretched more than its contour length, which implies $\nu_{\text{path}} \leq 1$, but it cannot also be more compact than Gaussian, meaning $\nu_{\text{path}} \geq 1/2$. These two conditions determine lower and upper critical dimensions, respectively:

$$\frac{p-\rho-x}{\rho(p-1)} \leq d \leq \frac{2(p-x)}{\rho(p-1)}. \quad \text{(13c)}$$

Above upper critical dimension excluded volume interactions become unimportant, meaning $\nu_{\text{path}} = 1/2$ and $\nu = \rho/2$. On the other hand, below lower critical dimension, chemical paths are completely stretched, $\nu_{\text{path}} = 1$, while overall molecule size is such that $\nu = \rho$. An additional peculiarity of quenched branched systems is that they cannot exist at all in space dimensions such that $\nu = \rho < 1/d$: their linear portions are already completely stretched, and they lack any means to resolve frustrations arising from the interplay of excluded volume and chain connectivity.

3.3.2 Annealed branching polymer—For branching polymers with annealed connectivity, the free energy per chain includes elastic contribution, Eq. (9), and interaction term, Eq. (12). Minimizing the sum with respect to R and using also Eqs. (10) and (11) we find

$$\nu = \frac{1+3(p-x)}{3(p-1)d+4}, \quad \text{(14a)}$$

$$\rho = \frac{(p-1)d+2(p-x+1)}{3(p-1)d+4}, \quad \text{(14b)}$$

$$\nu_{\text{path}} = \frac{1+3(p-x)}{(p-1)d+2(p-x+1)}. \quad \text{(14c)}$$

Implementing again the conditions $\nu_{\text{path}} \leq 1$ and $\nu_{\text{path}} \geq 1/2$, we can determine upper and lower critical dimensions:

$$1 - \frac{x}{p-1} \leq d \leq 4\frac{p-x}{p-1}. \quad \text{(14d)}$$

As in the quenched case, if d is above upper critical dimension, the role of excluded volume is marginal and the system connectivity is completely random, with $\nu = 1/4$, $\rho = 1/2$, and $\nu_{path} = 1/2$. The situation at the lower critical dimension for the annealed branching polymer is dramatically different from the quenched case. Annealed tree at low dimension d not only stretches its linear sections, but also rearranges its connectivity, increasing L, or increasing ρ. As a result, lower critical dimension corresponds to the situation when not only $\nu_{path} = 1$ (stretched linear sections), but also $\rho = 1$ (the tree is effectively simplified to become a linear trunk) and $\nu = 1$ (the whole molecule is stretched).

Below, we will explicitly consider various specific cases. All results are summarized in Fig. 3.

3.4 Isolated trees in a good solvent

3.4.1 Quenched case—A single macromolecule in a dilute solution in a good solvent corresponds to $p = 2$ (two-body repulsion) and $x = 0$ (no screening). In this case

$$\nu = \frac{2+\rho}{d+2}, \quad (15a)$$

$$\nu_{\mathrm{path}} = \frac{2+\rho}{\rho(d+2)}, \quad (15b)$$

with critical dimensions

$$\frac{2}{\rho} - 1 \leq d \leq \frac{4}{\rho}. \quad (15c)$$

Importantly, ρ here is controlled by how the molecule was prepared.

For instance, $\rho = 1$ corresponds to linear chains, and indeed Eqs. (15a)-(15c) reduce in this case to the classical Flory result (solid green line in Fig. 3, top left panel):

$$\nu = \nu_{\mathrm{path}} = \frac{3}{d+2}, \quad (16)$$

in $1 \leq d \leq 4$ dimensions.

For random trees with quenched ideal connectivity, $\rho = 1/2$, one recovers the Isaacson and Lubensky[11] prediction

$$\nu=\frac{5}{2d+4}, \quad (17a)$$

$$\nu_{\mathrm{path}}=\frac{5}{d+2}, \quad (17b)$$

$$3 \leq d \leq 8. \quad (17c)$$

In $d > 8$, excluded volume becomes insignificant, with $\nu_{\mathrm{path}} = 1/2$, leading to $\nu = 1/4$. Conversely, in $d \leq 3$ linear paths are completely stretched, with $\nu_{\mathrm{path}} = 1$, and molecule size is entirely controlled by its connectivity, with $\nu = \rho = 1/2$, as shown by the solid green line in Fig. 3 (middle and bottom left panels). Note that this line ends at $d = 2$ and does not continue to lower d. In fact, a quenched branched polymer with $\rho = 1/2$ faces and unresolvable frustration between excluded volume and chain connectivity requirements and can not exist in spaces with dimension lower than $d = 2$.

3.4.2 Annealed case—For a single ($x = 0$, no screening) swollen randomly branching polymers with annealed connectivity in a good solvent ($p = 2$), Eqs. (14a)-(14d) reduce to the prediction of Gutin *et al.* [38]:

$$\nu=\frac{7}{3d+4}, \quad (18a)$$

$$\rho=\frac{d+6}{3d+4}, \quad (18b)$$

$$\nu_{\mathrm{path}}=\frac{7}{d+6}, \quad (18c)$$

$$1 \leq d \leq 8. \quad (18d)$$

For annealed trees, the limit of full path stretching is only reached in $d = 1$ dimensions, where $\nu = \rho = \nu_{\mathrm{path}} = 1$. The results for the isolated annealed branching polymer in a good solvent are depicted by the green solid lines in Fig. 3 (right panels).

3.5 Isolated trees in a θ-solvent

3.5.1 Quenched case—For the case of dilute solutions ($x = 0$, no screening) in a θ-solvent ($p = 3$, three-body repulsion, because $\nu_2 = 0$) we have:

$$\nu=\frac{3+\rho}{2(d+1)}, \quad (19a)$$

$$\nu_{\mathrm{path}}=\frac{3+\rho}{2\rho(d+1)}, \quad (19b)$$

$$\frac{3-\rho}{2\rho} \leq d \leq \frac{3}{\rho}. \quad (19c)$$

For linear chains with $\rho = 1$ (solid magenta line in Fig. 3, top left panel):

$$\nu=\frac{2}{d+1} \quad (20)$$

and the three-body repulsion is only relevant for $d < 3$ dimensions, while chains become fully stretched in $d = 1$ and cannot exist in $d < 1$ because of the frustration between excluded volume and chain connectivity.

For trees with ideal connectivity, $\rho = 1/2$, one recovers:

$$\nu=\frac{7}{4(d+1)}, \quad (21a)$$

$$\nu_{\mathrm{path}}=\frac{7}{2(d+1)}, \quad (21b)$$

$$\frac{5}{2} \leq d \leq 6. \quad (21c)$$

corresponding to the result by Daoud and Joanny[33]. The statistics of linear paths suggests that linear sections of the polymer become fully stretched for $d \leq 5/2$ and $\nu = \rho = 1/2$, as

shown in the middle and bottom left panels of Fig. 3 in solid magenta lines. As in good solvent solutions, randomly branched polymers with $\rho = 1/2$ in θ-solutions do not fit in spaces with dimensionality below $d = 2$.

3.5.2 Annealed case—For trees with annealed connectivity, Eqs. (14a) to (14b) reduce to

$$\nu=\frac{5}{3d+2}, \quad (22a)$$

$$\rho=\frac{d+4}{3d+2}, \quad (22b)$$

$$\nu_{\mathrm{path}}=\frac{5}{d+4}, \quad (22c)$$

$$1 \leq d \leq 6. \quad (22d)$$

To the best of our knowledge these relations have not been reported in the literature before and are plotted as magenta lines in Fig. 3 (right panels).

3.6 Melts of branched or branching polymers

3.6.1 Quenched case—Eqs. (13a)-(13b) can also be applied to melts of branched polymers. In melts, volume interactions are screened implying that $x = 1$ in the virial-type expansion of the interaction energy term, Eq. (12) [11,18], which becomes $\frac{\mathscr{F}_{\mathrm{inter}}^{(p,x=1)}}{k_B T} \sim \nu_p \left(\frac{N}{R^d}\right)^{p-1}$. Close inspection to these terms shows that interactions are estimated to be irrelevant, if $\nu d > 1$. Even without swelling, this is the case in $d > 4$ dimensions, where $\nu^{ideal} d = d/4 > 1$ suggests ideal tree behavior. Conversely, in $d \leq 4$ dimensions, for $1/4 < \nu \leq 1/d$ all terms of the series need to be taken into account, implying that the series is dominated by high-order interactions with $p \to \infty$[33]. In particular, the $p \to \infty$ limit of Eqs. (13a)-(13b) gives:

$$\nu=\frac{1}{d}, \quad (23a)$$

$$\nu_{\mathrm{path}}=\frac{1}{d\rho}, \quad (23b)$$

$$\frac{1}{\rho}\leq d\leq\frac{2}{\rho}. \quad (23c)$$

The $\nu = 1/d$ result means that trees in the melt are "territorial"[30,73], and each of them behaves as a compact object. As before, ρ is the property of the system in question. For instance, for the melt of linear chains, $\rho = 1$, the interval between lower and upper critical dimension, $1 \leq d \leq 2$, does not include 3 (solid blue line in the top left panel of Fig. 3); that means the well known textbook fact that linear chains in a regular $3d$ melt are approximately Gaussian (Flory theorem). At dimensions below 2 they swell, at $d = 1$ they are completely stretched, and cannot be placed in $d < 1$.

In contrast to linear chains, randomly branched polymers with ideal connectivity $\rho = 1/2$ in the regular $3d$ melt are "territorial"[73], they do not obey Flory theorem and their linear sub-chains are predicted to exhibit a non-trivial statistics. The results for quenched tree melts are shown as solid blue lines in the middle and bottom left panels of Fig. 3. As before, the lines stop at $d = 2$, because quenched polymer cannot be placed in space of lower dimension.

3.6.2 Annealed case—For trees with annealed connectivity, screening is still important, meaning $x = 1$, as well as many-body interactions, suggesting again the limit $p \to \infty$. The results read:

$$\nu=\frac{1}{d}, \quad (24a)$$

$$\rho=\frac{d+2}{3d}, \quad (24b)$$

$$\nu_{\mathrm{path}}=\frac{3}{d+2}, \quad (24c)$$

$$1\leq d\leq 4. \quad (24d)$$

Interestingly, territorial behavior with $\nu = 1/3$ is expected for both, randomly branched and randomly branching, polymers in $d = 3$. However, the annealed trees are expected to be less

strongly branched, $\rho = 5/9 > 1/2$, with less strongly stretched linear paths, $\nu_{path} = 3/5 < 2/3$[18]. The results for annealed tree melt are given as solid blue lines in Fig. 3 (right panels).

3.7 Examples of other preparation protocols

We emphasized repeatedly that connectivity of a quenched polymer, described by L or ρ, is controlled by the preparation conditions, but we explicitly considered only two examples: $\rho = 1$ (linear polymer) and $\rho = 1/2$ (ideally branched polymer). Let us give a couple more examples and illustrate the application of our results.

Suppose we prepare (synthesize) branched polymer in a θ-solvent, then quench its connectivity, and then change solvent quality to good while keeping the solution very dilute. We have everything to describe this situation. Since the molecule is prepared in a θ-solvent, its connectivity is annealed under θ-conditions and, therefore, it is characterized by index ρ given in Eq. (22b) at $d = 3$, namely $\rho = 7/11$. Now, with this value of ρ fixed, the molecule is placed in good solvent conditions. We thus have to insert $\rho = 7/11$ into Eqs. (15a) and (15b) to obtain $\nu = 29/55 \approx 0.53$ and $\nu_{path} = 29/35 \approx 0.83$. We see that linear sections of the tree are significantly stretched, which is natural given how this tree was prepared.

As a second example, suppose we prepare branched polymers in a good solvent, quench their connectivity, and then concentrate the resulting macromolecules to form a melt. To describe this situation, we first look at Eq. (18b) at $d = 3$, and find that the molecule in a good solvent will have $\rho = 9/13$. In this case, the space dimension $d = 3$ is above upper critical for melts, which is (see Eq. (23c)) $2/\rho = 26/9 \approx 2.89$. As a consequence, such melts are expected to be ideal with $\nu_{path} = 1/2$ and $\nu = \rho/2$.

In a similar way we can consider also many other preparation protocols. Curiously, it should not be possible to generate randomly branched polymers with quenched *ideal* statistics *along these lines*: in $d \leq 3$ all annealed branching systems exhibit swelling with $\rho > 1/2$.

4 Comparison of Flory Theory predictions to theoretical and simulation results

Flory theory[37] owes its simplicity to uncontrolled approximations, the neglect of spatial correlations arising from the connectivity of the chains and to Gaussian estimate of polymer elasticity. To gauge the utility of the approach, its predictions need to be compared to exact solutions [14,44,46,47], ε-expansions [39] renormalisation group calculations [14,40,41,43,49], dimensional reduction[45], series expansions[16,48] exact enumerations[42,50–52,54], Monte Carlo [53,55–63] and Molecular Dynamics [62] simulations. Tables 1 to 4 list available benchmark results for linear chains and for trees with annealed and with quenched ideal connectivity. Typically, analytical approaches only provide access to the overall asymptotic behaviour as characterised by the exponent ν. In contrast, numerical investigations extract estimates for ν, ρ, and ν_{path} from data for polymers of finite size.

To set the stage, let us briefly review the situation for linear chains. The results presented in Table 1 show that Flory theory works remarkably well, with the only exception of $2d$ chains in θ-solvent. The theory correctly predicts (i) $\nu = 1$ for all interacting systems in $d = 1$, (ii)

the hierarchy $\nu_{SAW} \geq \nu_{\theta} \geq \nu_{melt}$ for all d, and (iii) the upper critical dimensions $d_{SAW} = 4$, $d_{\theta} = 3$, and $d_{melt} = 2$ for the three media types. The values of the predicted exponents are mostly exact. Exceptions are self-avoiding walks in $d = 3$ dimensions, where the Flory estimate of $\nu_F = 3/5$ slightly exceeds the best estimates[40] of $\nu \approx 0.588$, and linear chains in θ-solvents in $d = 2$, where the deviation between the Flory estimate, $\nu_F = 2/3$, and the exact value of $\nu = 4/7$[47] is larger.

A first, visual inspection of the values listed in Tables 2 to 4 suggests that Flory theory works almost as well for trees as for linear chains. This is confirmed by Figure 3, where we compare the results (symbols) to the predictions of Flory theory (lines) for the relevant exponents ν, ρ, and ν_{path} as a function of dimension, d. Different sets of panels are devoted to linear chains, trees with quenched ideal connectivity and trees with annealed connectivity. The theory correctly predicts (i) $\nu = 1$ for all types of annealed trees in $d = 1$, (ii) the hierarchy $\nu_{SAW} \geq \nu_{\theta} \geq \nu_{melt}$ for all d, and (iii) the upper critical dimensions $d_{SAW} = 8$, $d_{\theta} = 6$, and $d_{melt} = 4$ for the three solution types. Moreover, all known values for the exponents fall in between these bounds, see Tables 1–4. In spite of its simplicity, it is indeed quite remarkable that Flory theory correctly anticipates all observed trends.

The key element of the Flory theory for annealed trees is the description of the tree elasticity summarised in Sec. 3.1.2, which implies that the swelling of annealed trees results from a *combination* of modified branching and path stretching. This and the dominance of the path stretching mode (Sec. 3.2) are qualitatively confirmed by the benchmark results wherever independent information is available for the exponents ρ or ν_{path}. Interestingly, the benchmark results are in good agreement with the predicted relations, Eqs. (10) and (11), between the exponents for annealed trees (Fig. 4). The same holds for the comparison of annealed trees and trees with quenched *ideal* connectivity, $\rho = 1/2$. The latter are predicted to exhibit *less* overall swelling than trees with annealed connectivity, even though they are expected to be stretched *more strongly* on the path level (Eqs. (17a) and (17b) vs. Eqs. (18a) and (18c)). These features are directly observed in numerical simulations[58,62] and confirm that trees with annealed and quenched ideal connectivity fall into different universality classes[38].

Nevertheless, Flory theory is no more exact for trees than for linear chains. For instance, there is a tendency to overestimate the exponent ν in good and θ-solvents. For example, Flory theory predicts $\nu = 7/13$ instead of the exact result[14] $\nu = 1/2$ for self-avoiding trees with annealed connectivity in $d = 3$ dimensions. The absolute deviations is much larger for trees (0.038) than for linear chains (0.012), but the relative errors of the predicted effects, $(7/13 - 1/2)/(1/2 - 1/4) = 15\%$ and $(3/5 - 0.588)/(0.588 - 1/2) \approx 14\%$, are of comparable magnitude. Another example are annealed branching polymers in dilute θ-solutions in $d = 2$ dimensions. Flory theory predicts $\nu = 5/8$ instead of the best numerical result[61] 0.5359 ± 0.0003 for trees with annealed connectivity. In this case, the absolute errors are comparable for annealed trees (0.089) and linear chains (0.095), but the relative error for annealed trees, $(5/8 - 0.5359)/(0.5359 - 1/4) = 31\%$, is much *smaller* than for linear chains, where Flory theory is off by $(2/3 - 4/7)/(4/7 - 1/2) \approx 133\%$.

5 Summary and conclusion

In the present article, we have reviewed the Flory theory of branched polymers with volume interactions as pioneered in Refs.[11,18,33,38] and completed the theory for the case of annealed branching polymers in dilute θ-solvent solutions. An important point is the distinction[38] between annealed and quenched trees. To reduce the number of unfavorable contacts, the latter can only swell by modifying the conformational statistics of linear paths to values $\nu_{path} > 1/2$ (Fig. 3, middle panels). The former have the additional option to increase their overall size by adjusting the branching statistics, $\rho > 1/2$ (Fig. 3, right panels). The predicted behaviour for trees is considerably richer than for linear chains [75], which represent the limiting case of trees with quenched connectivity characterised by $\rho = 1$ (Fig. 3, left panel).

The predictions of Flory theory are shown to be in excellent qualitative agreement with available theoretical and numerical results (compare symbols to solid lines in Figs. 3 and 4). While quantitative predictions from Flory theory need to be taken with a grain of salt, the approach thus provides a simple and unifying description of the average swelling behaviour of a wide range interacting tree systems.

However, there are other quantities such as entropies[60] and internodal contact probabilities[62,63], which Flory theory fails to describe even for linear chains[75]. A forthcoming article[76] discusses how to go beyond Flory theory and the Gaussian approximation by analyzing the distribution functions characterising the tree conformations and connectivity.

Acknowledgments

RE, MR, and AYG are grateful for the hospitality of the Kavli Institute for Theoretical Physics (Santa Barbara, USA) and support through the National Science Foundation under Grant No. NSF PHY11-25915 during their visit in 2011. AR acknowledges grant PRIN 2010HXAW77 (Ministry of Education, Italy). MR acknowledges financial support from the National Science Foundation under grants DMR-1309892, DMR-1436201, and DMR-1121107, the National Institute of Health under grants P01-HL108808 and 1UH2HL123645, and the Cystic Fibrosis Foundation.

References

1. Rubinstein, M., Colby, RH. Polymer Physics. Oxford University Press; New York: 2003.
2. Burchard W. Adv Polym Sci. 1999; 143:113.
3. Bacova P, Hawke LGD, Read DJ, Moreno AJ. Macromolecules. 2013; 46:4633–4650.
4. Zimm BH, Stockmayer WH. J Chem Phys. 1949; 17:1301–1314.
5. Stauffer, D., Aharony, A. Introduction to percolation theory. Taylor & Francis Inc; 1994.
6. Liu L, Hyeon C. Biophys J. 2016; 110:2320. [PubMed: 27276250]
7. Kelly J, Grosberg AY, Bruinsma R. J Phys Chem B. 2016; 120:6038–6050. [PubMed: 27116641]
8. Singaram SW, Gopal A, Ben-Shaul A. J Phys Chem B. 2016; 120:6231–6237. [PubMed: 27104292]
9. Marko J, Siggia E. Phys Rev E. 1995; 52:2912–2938.
10. Mondal J, Bratton BP, Li Y, Yethiraj A, Weisshaar JC. Biophys J. 2011; 100:2605–2613. [PubMed: 21641305]
11. Isaacson J, Lubensky TC. J Physique Lett. 1980; 41:469–471.
12. Seitz WA, Klein DJ. J Chem Phys. 1981; 75:5190–5193.
13. Duarte J, Ruskin H. J Physique. 1981; 42:1585–1590.

14. Parisi G, Sourlas N. Phys Rev Lett. 1981; 46:871–874.
15. Fisher M. Phys Rev Lett. 1978; 40:1610–1613.
16. Kurtze D, Fisher M. Phys Rev B. 1979; 20:2785–2796.
17. Bovier, A., Fröhlich, J., Glaus, U. Branched Polymers and Dimensional Reduction. In: Osterwalder, K., Stora, R., editors. Critical Phenomena, Random Systems, Gauge Theories. North-Holland, Amsterdam: 1984.
18. Grosberg AY. Soft Matter. 2014; 10:560–565. [PubMed: 24652534]
19. Rosa A, Everaers R. Phys Rev Lett. 2014; 112:118302. [PubMed: 24702424]
20. Ge T, Panyukov S, Rubinstein M. Macromolecules. 2016; 49:708–722. [PubMed: 27057066]
21. Khokhlov AR, Nechaev SK. Phys Lett. 1985; 112A:156–160.
22. Rubinstein M. Phys Rev Lett. 1986; 57:3023–3026. [PubMed: 10033934]
23. Obukhov SP, Rubinstein M, Duke T. Phys Rev Lett. 1994; 73:1263–1266. [PubMed: 10057666]
24. Michieletto D, Turner MS. Proc Natl Acad Sci USA. 2016; 113:5195–5200. [PubMed: 27118847]
25. Michieletto D. Soft Matter. 2016; 12:9485–9500. [PubMed: 27781227]
26. Grosberg A, Rabin Y, Havlin S, Neer A. Europhys Lett. 1993; 23:373–378.
27. Rosa A, Everaers R. Plos Comput Biol. 2008; 4:e1000153. [PubMed: 18725929]
28. Vettorel T, Grosberg AY, Kremer K. Phys Biol. 2009; 6:025013. [PubMed: 19571364]
29. Mirny LA. Chromosome Res. 2011; 19:37–51. [PubMed: 21274616]
30. Halverson JD, Smrek J, Kremer K, Grosberg AY. Rep Prog Phys. 2014; 77:022601. [PubMed: 24472896]
31. Kerpedjiev P, Hammer S, Hofacker IL. Bioinformatics. 2015; 31:3377–3379. [PubMed: 26099263]
32. De Gennes PG. Biopolymers. 1968; 6:715. [PubMed: 5648278]
33. Daoud M, Joanny JF. J Physique. 1981; 42:1359–1371.
34. des Cloizeaux, J., Jannink, G. Polymers in Solution. Oxford University Press; Oxford: 1989.
35. Grosberg, AY., Khokhlov, AR. Statistical Physics of Macromolecules. AIP Press; New York: 1994.
36. De Gennes PG. J Physique Lett. 1976; 37:L59–L61.
37. Flory, PJ. Principles of Polymer Chemistry. Cornell University Press; Ithaca (NY): 1953.
38. Gutin AM, Grosberg AY, Shakhnovich EI. Macromolecules. 1993; 26:1293–1295.
39. De Gennes PG. J Physique Lett. 1975; 36:L55–L57.
40. Le Guillou JC, Zinn-Justin J. Phys Rev Lett. 1977; 39:95–98.
41. Family F. J Phys A-Math Gen. 1980; 13:L325–L334.
42. de Alcantara OF, Kirkham JE, McKane AJ. J Phys A-Math Gen. 1980; 13:L247–L251.
43. Derrida B, de Seze L. J Physique. 1982; 43:475–483.
44. Nienhuis B. Phys Rev Lett. 1982; 49:1062–1065.
45. Dhar D. Phys Rev Lett. 1983; 51:853–856.
46. Duplantier B. J Phys A-Math Gen. 1986; 19:L1009.
47. Duplantier B, Saleur H. Phys Rev Lett. 1987; 59:539–542. [PubMed: 10035800]
48. Adler J, Meir Y, Harris A, Aharony A, Duarte J. Phys Rev B. 1988; 38:4941–4954.
49. Janssen HK, Stenull O. Phys Rev E. 2011; 83:051126.
50. Gaunt DS, Sykes MF, Torrie GM, Whittington SG. J Phys A-Math Gen. 1982; 15:3209–3217.
51. Privman V. Physica A. 1984; 123:428–442.
52. Margolina A, Family F, Privman V. Z Phys B-Condens Mat. 1984; 54:321–324.
53. Meirovitch H. J Phys A-Math Gen. 1987; 20:6059–6073.
54. Ishinabe T. J Phys A-Math Gen. 1989; 22:4419–4431.
55. Janse van Rensburg EJ, Madras N. J Phys A: Math Gen. 1992; 25:303–333.
56. Li B, Madras N, Sokal AD. J Stat Phys. 1995; 80:661–754.
57. Wittkop M, Kreitmeier S, Göritz D. J Chem Phys. 1996; 104:3373–3385.
58. Cui S, Chen Z. Phys Rev E. 1996; 53:6238–6243.
59. Madras N, Janse van Rensburg EJ. J Stat Phys. 1997; 86:1–36.

60. Hsu HP, Nadler W, Grassberger P. J Phys A: Math Gen. 2005; 38:775.
61. Hsu HP, Grassberger P. J Stat Mech: Theory Exp. 2005; 2005:P06003.
62. Rosa A, Everaers R. J Phys A: Math Theor. 2016; 49:345001.
63. Rosa A, Everaers R. J Chem Phys. 2016; 145:164906. [PubMed: 27802612]
64. Bhattacharjee SM, Giacometti A, Maritan A. J Phys: Condens Matter. 2013; 25:503101. [PubMed: 24222476]
65. Daoud M, Cotton JP. J Phys France. 1982; 43:531–538.
66. Raphael E, Pincus P, Fredrickson GH. Macromolecules. 1993; 26:1996–2006.
67. Boris D, Rubinstein M. Macromolecules. 1996; 29:7251–7260.
68. Kröger M, Peleg O, Halperin A. Macromolecules. 2010; 43:6213–6224.
69. Daoud M, Pincus P, Stockmayer WH, Witten T. Macromolecules. 1983; 16:1833–1839.
70. Doi, M., Edwards, SF. The Theory of Polymer Dynamics. Oxford University Press; New York: 1986.
71. Grosberg AY, Nechaev SK. J Phys A-Math Theor. 2015; 48:345003.
72. Smrek J, Grosberg AY. J Phys: Condens Matter. 2015; 27:064117. [PubMed: 25563563]
73. Vettorel T, Grosberg AY, Kremer K. Phys Today. 2009; 62:72.
74. Flory, PJ. Statistical Mechanics of Chain Molecules. Interscience; New York: 1969.
75. De Gennes, PG. Scaling Concepts in Polymer Physics. Cornell University Press; Ithaca: 1979.
76. Rosa, A., Everaers, R. Phys Rev E. 2017. accepted for publication Preprint: http://arxiv.org/abs/1610.05230

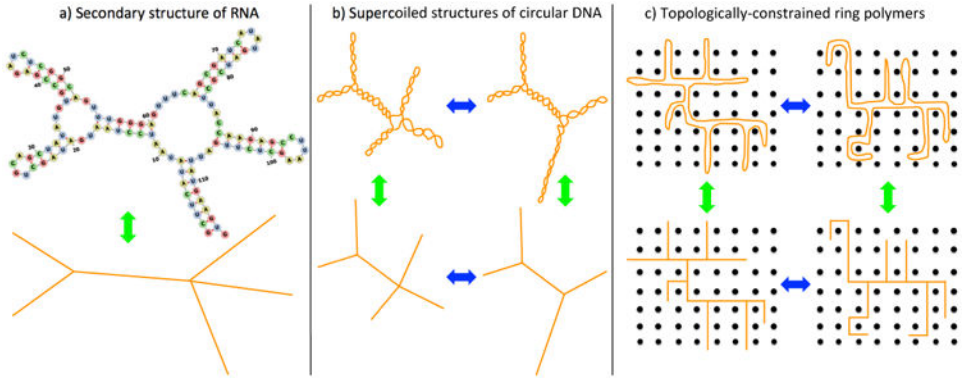

Fig. 1.

(a) Due to the Watson-Crick base pair mechanism and neglecting the difference of excluded volumes between loops and stems, single filaments of RNA have a branched secondary structure (here, visualized by the FORNA[31] software). These structures have been shown[6–8] to play a crucial functional role in the RNA behavior inside viral capsids. (b) The increase of the level of supercoiling in circular polymers (rings) gives rise to the formation of plectonemes: by neglecting plectonemes torsional properties, rings assume the shape of branched structures[9] which reproduce the experimental behaviour of circular DNA inside the bacterial nucleoid[10]. According to the total amount and distribution of supercoiling the ring may continuously switch between different branched structures. (c) By neglecting the excluded volume interactions between double-folded strands, a single ring polymer constrained in a matrix of fixed obstacles[21–23] resembles a branched polymer with annealed connectivity: in this situation, an “elk” may change into a “camel” and viceversa.

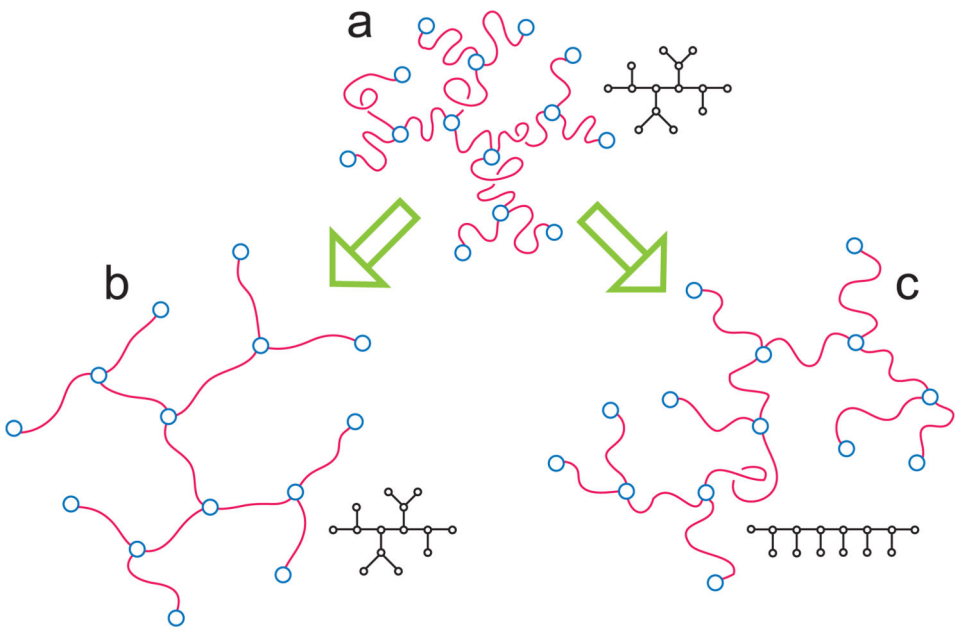

Fig. 2.

Schematic representation of the two independent swelling mechanisms for interacting trees (a). (b) With *quenched* connectivity, branched polymers can swell only by stretching its linear sections. (c) With *annealed* connectivity, in addition to stretching linear sections, branching polymers can also simplify the connectivity which can become somewhat “less branched” as, for instance, in the combo-like conformation shown in the picture. Then, to achieve the same overall swelling, an annealed tree has to stretch its linear sections by a lesser amount than the quenched counterpart.

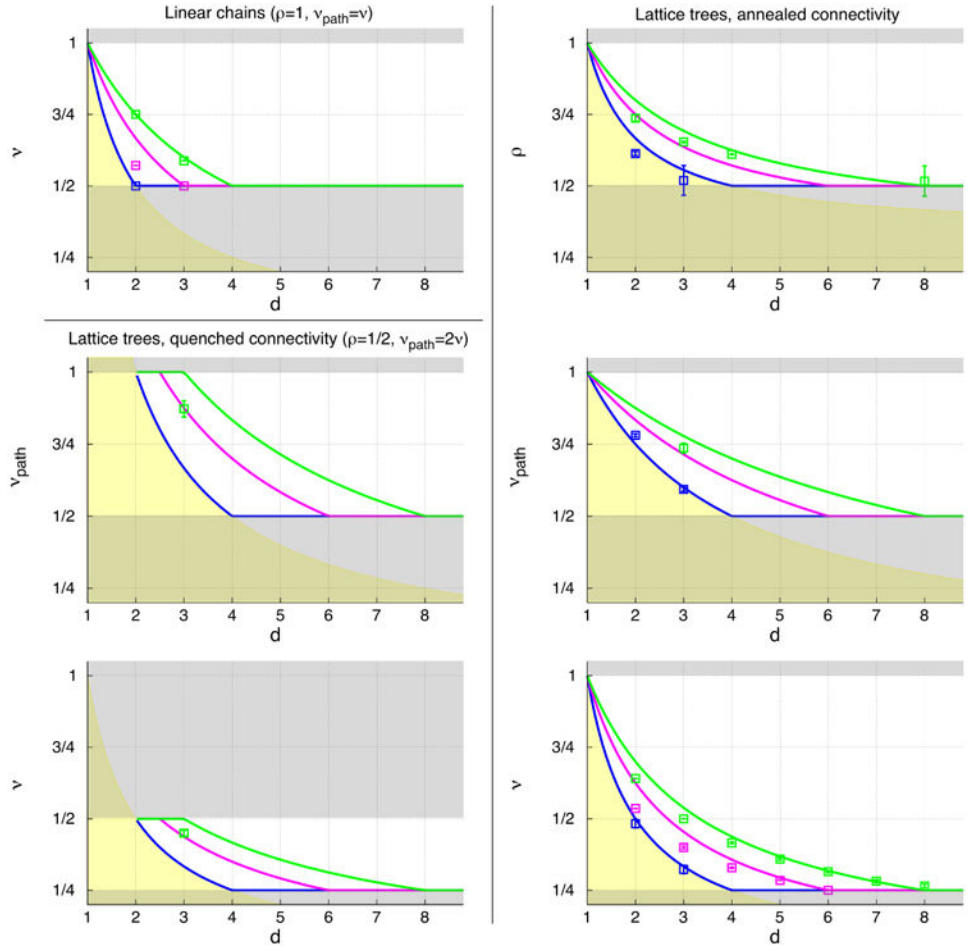

Fig. 3.

Exponents ρ, ν_{path} and ν for: linear chains (upper panel on the left, $\rho = 1$ and $\nu_{\text{path}} = \nu$), trees with quenched ideal connectivity (middle and bottom panels on the left, $\rho = 1/2$), trees with annealed connectivity (panels on the right). Solid lines correspond to predictions of Flory theory: green is for single chains in good solvent (Eq. (16) for linear chains, Eqs. (17a)-(17b) for quenched trees and Eqs. (18a)-(18c) for annealed trees); magenta is for single chains in θ-solvent (Eq. (20) for linear chains, Eqs. (21a)-(21b) for quenched trees and Eqs. (22a)-(22c) for annealed trees); blue is for chains in melt (Eqs. (23a)-(23b) for, respectively, linear chains and quenched trees with ideal connectivity and Eqs. (24a)-(24c) for annealed trees). Grey- and yellow-shading regions indicate violations of the following physical constraints on the values of the exponents: (grey) $1/2 \le \rho \le 1$, $1/2 \le \nu_{\text{path}} \le 1$ and $1/4 \le \nu \le 1$ for lattice trees and $1/2 \le \nu \le 1$ for linear chains; (yellow) the fractal dimension $d_f = 1/\nu$ of any object placed in space must be $\le d$. For annealed trees, given Eqs. (4), (10) and (11), constraints for one exponent map to the corresponding constraints for the others. This is not the case for quenched trees, where constraints for ν_{path} restrict corresponding values of ν to a narrower region. Symbols are for computer simulations and analytical results boldfaced in Tables 1–4.

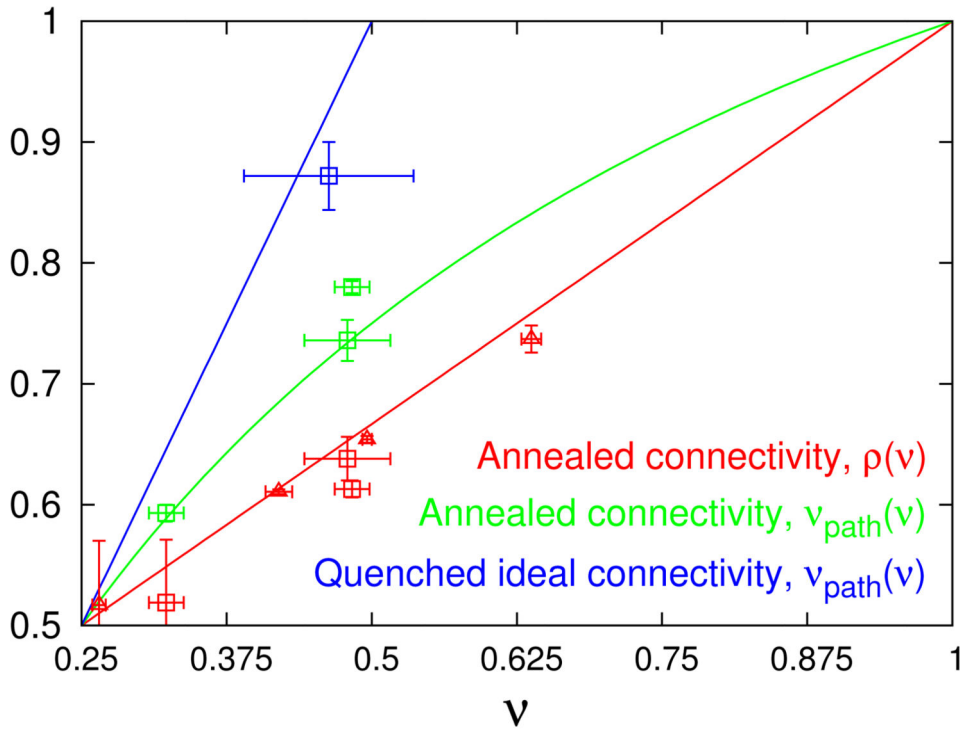

Fig. 4.

Exponents ρ and ν_{path} are plotted as a function of ν following the expressions Eqs. (10), (11) for annealed trees (red and green lines) and $\nu_{\text{path}}=\frac{\nu}{\rho}$ with $\rho = 1/2$ (blue line) for trees with quenched ideal connectivity. Symbols correspond to numerical results for: (triangles) annealed dilute trees in good solvent in $d = 2,3,4,8$[55]; (squares) annealed and quenched dilute trees in good solvent in $d = 3$[62] and annealed tree melts in $d = 2,3$[63].

Table 1

Analytical and simulation results for critical exponent ν of linear chains ($\rho = 1$, $\nu_{\text{path}} = \nu$) for different solvent conditions and spatial dimensionality d. "$\frac{\delta\nu}{\delta\nu_{\text{ideal}}} \equiv \frac{\nu - \nu_{\text{true}}}{\nu_{\text{true}} - \nu_{\text{ideal}}} \times 100$ is the relative discrepancy between the *actual* and the *true* values (in boldface) of ν over the difference between the latter and the *ideal* value. Currently available exact values or best estimates (in boldface) are reported as symbols in Fig. 3, where predictions of Flory theory are shown as lines.

Linear chains					
d	$\boldsymbol{\nu}$	$\boldsymbol{\delta\nu}$	$\frac{\delta\nu}{\delta\nu_{\text{ideal}}}$	**Technique**	**Reference**
Dilute solution in a good solvent					
2	3/4 = 0.75	0	0%	Flory theory	Flory (1969)[74]
2	**3/4 = 0.75**	–	–	Exact calculation	Nienhuis (1982)[44]
2	0.74963±0.00008	−0.00037	−0.2%	Monte Carlo	Li, Madras & Sokal (1995)[56]
3	3/5 = 0.6	0.0123	14%	Flory theory	Flory (1969)[74]
3	0.588±0.001	0.0003	0.3%	Renormalization group	Le Guillou & Zinn-Justin (1977)[40]
3	**0.5877±0.0006**	–	–	Monte Carlo	Li, Madras & Sokal (1995)[56]
Dilute solution in a θ-solvent					
2	2/3 = 0.667	0.0952	133%	Flory theory	Flory (1969)[74]
2	367/726 ≈ 0.5055	−0.0659	-92%	ϵ-expansion	De Gennes (1975)[39]
2	**4/7 ≈ 0.5714**	–	–	Exact calculation	Duplantier & Saleur (1987)[47]
2	0.57±0.02	−0.0014	-2%	Monte Carlo	Wittkop, Kreitmeier & Göritz (1996)[57]
3	1/2 = 0.5	0	0%	Flory theory	Flory (1969)[74]
3	**1/2 = 0.5**	–	–	ϵ-expansion	De Gennes (1975)[39]
3	0.50±0.02	0.00	0%	Monte Carlo	Wittkop, Kreitmeier & Göritz (1996)[57]
Melt					
2	1/2 = 0.5	0	0%	Flory theory	Isaacson & Lubensky (1980)[11]
2	**1/2 = 0.5**	–	–	Conformal theory	Duplantier (1986)[46]

Linear chains

d	ν	$\delta\nu$	$\frac{\delta\nu}{\delta\nu_{\mathrm{ideal}}}$	Technique	Reference
3	1/2 = 0.5	–	–	Flory theory	Isaacson & Lubensky (1980)[11]

Table 2

Analytical and simulation results for critical exponents ρ, ν_{path} and ν of isolated self-avoiding lattice trees in a good solvent for different spatial dimensionalities d. $\frac{\delta\nu}{\delta\nu_{\text{ideal}}}$ is defined as in Table 1. Currently available exact values or best estimates (in boldface) are reported as symbols in Fig. 3, where predictions of Flory theory are shown as lines.

Annealed branching polymers in dilute solutions in a good solvent

d	ρ	ν_{path}	ν	$\delta\nu$	$\frac{\delta\nu}{\delta\nu_{\text{ideal}}}$	Technique	Reference
2	4/5=0.8	7/8=0.875	7/10 = 0.7	0.0592	15%	Flory theory	Gutin *et al.* (1993)[38]
2	–	–	0.637	−0.0038	-1%	Renormalization group	Family (1980)[41]
2	–	–	**0.6408 ±0.0003**	–	–	Renormalization group	Derrida & de Seze (1982)[43]
2	–	–	0.640 ±0.004	−0.0008	-0.2%	Exact enumeration	Margolina *et al.* (1984)[52]
2	–	–	0.6394 ±0.0067	−0.0014	-0.4%	Exact enumeration	Privman (1984)[51]
2	–	–	0.640 ±0.004	−0.0008	-0.2%	Scanning method	Meirovitch (1987)[53]
2	–	–	0.644 ±0.004	0.0032	0.8%	Exact enumeration	Ishinabe (1989)[54]
2	**0.74 ±0.01**	–	0.637 ±0.009	−0.0038	-1%	Monte Carlo	J. van Rensburg & Madras (1992)[55]
2	–	–	0.6412±0.0005	0.0004	0.1%	Monte Carlo	Hsu *et al.* (2005)[60]
3	9/13=0.692	7/9=0.778	7/13 = 0.538	0.0385	15%	Flory theory	Gutin *et al.* (1993)[38]
3	–	–	**1/2**	–	–	Exact calculation	Parisi & Sourlas (1981)[14]
3	**0.654 ±0.003**	–	0.496 ±0.004	−0.004	-2%	Monte Carlo	J. van Rensburg & Madras (1992)[55]
3	–	–	0.49 ± 0.01	−0.01	-4%	Monte Carlo	Cui & Chen (1996)[58]
3	–	–	0.500 ±0.002	0.000	0%	Monte Carlo	Hsu *et al.* (2005)[60]
3	0.64±0.02	**0.74 ±0.02**	0.48 ±0.04	0.02	-8%	Monte Carlo	Rosa & Everaers (2016)[62]
4	5/8=0.625	7/10=0.7	7/16 = 0.438	0.022	13%	Flory theory	Gutin *et al.* (1993)[38]
4	–	–	0.425	0.009	5%	Series expansion	Kurtze & Fisher (1979)[16]
4	–	–	0.450 ±0.035	0.034	21%	Exact enumeration	de Alcantara *et al.* (1980)[42]
4	–	–	0.42	0.04	2%	Renormalization group	Parisi & Sourlas (1981)[14]
4	–	–	0.45 ±0.05	0.034	21%	Exact enumeration	Gaunt *et al.* (1982)[50]
4	–	–	0.417	0.001	0.6%	Dimensional reduction	Dhar (1983)[45]

Annealed branching polymers in dilute solutions in a good solvent

d	ρ	ν_{path}	ν	$\delta\nu$	$\frac{\delta\nu}{\delta\nu_{ideal}}$	Technique	Reference
4	–	–	0.425 ±0.015	0.009	5%	Series expansion	Adler *et al.* (1988)[48]
4	**0.611 ±0.002**	–	0.42±0.01	0.004	2%	Monte Carlo	J. van Rensburg & Madras (1992)[55]
4	–	–	**0.416 ±0.003**	–	–	Monte Carlo	Hsu *et al.* (2005)[60]
5	11/19=0.579	7/11=0.636	7/19 = 0.368	0.009	8%	Flory theory	Gutin *et al.* (1993)[38]
5	–	–	**0.359 ±0.004**	–	–	Monte Carlo	Hsu *et al.* (2005)[60]
6	6/11=0.545	7/12=0.583	7/22 = 0.318	0.003	5%	Flory theory	Gutin *et al.* (1993)[38]
6	–	–	**0.315 ±0.004**	–	–	Monte Carlo	Hsu *et al.* (2005)[60]
7	13/25=0.52	7/13=0.538	7/25 = 0.28	−0.002	-6%	Flory theory	Gutin *et al.* (1993)[38]
7	–	–	**0.282 ± 0.005**	–	–	Monte Carlo	Hsu *et al.* (2005)[60]
8	1/2=0.5	1/2=0.5	1/4 = 0.25	−0.015	−100%	Flory theory	Gutin *et al.* (1993)[38]
8	**0.52 ±0.05**	–	**0.265 ±0.006**	–	–	Monte Carlo	J. van Rensburg & Madras (1992)[55]

Quenched branched polymers in dilute solutions in a good solvent

d	ρ	ν_{path}	ν	$\delta\nu$	$\frac{\delta\nu}{\delta\nu_{ideal}}$	Technique	Reference
3	1/2	1	1/2 = 0.5	0.05	25%	Flory theory	Isaacson & Lubensky (1980)[11]
3	1/2	–	**0.45 ±0.01**	–	–	Monte Carlo	Cui & Chen (1996)[58]
3	1/2	**0.87 ±0.03**	0.46 ±0.07	0.01	5%	Molecular Dynamics	Rosa & Everaers (2016)[62]

Table 3

Analytical and simulation results for critical exponents ρ, ν_{path} and ν of annealed isolated self-avoiding lattice trees in a θ-solvent for different spatial dimensionalities d. $\frac{\delta\nu}{\delta\nu_{\text{ideal}}}$ is defined as in Table 1. Currently available exact values or best estimates (in boldface) are reported as symbols in Fig. 3, where predictions of Flory theory are shown as lines. To our knowledge, analytical or simulation data for quenched isolated branched polymers in θ-solutions are currently missing.

Annealed branching polymers in dilute solutions in a θ-solvent

d	ρ	ν_{path}	ν	$\delta\nu$	$\frac{\delta\nu}{\delta\nu_{\text{ideal}}}$	Technique	Reference
2	3/4=0.75	5/6=0.833	5/8 = 0.625	0.0891	31%	Flory theory	This work
2	–	–	0.54±0.03	0.0041	1%	Monte Carlo	Madras & J. van Rensburg (1997)[59]
2	–	–	**0.5359±0.0003**	–	–	Monte Carlo	Hsu & Grassberger (2005)[61]
2	–	–	0.52±0.03	−0.0159	-6%	Renormalization group	Janssen & Stenull (2011)[49]
3	7/11=0.636	5/7=0.714	5/11 = 0.455	0.055	36%	Flory theory	This work
3	–	–	**0.400 ±0.005**	–	–	Monte Carlo	Madras & J. van Rensburg (1997)[59]
3	–	–	0.396 ±0.007	−0.004	-3%	Renormalization group	Janssen & Stenull (2011)[49]
4	4/7=0.571	5/8=0.625	5/14 = 0.357	0.028	35%	Flory theory	This work
4	–	–	**0.329 ± 0.002**	–	–	Renormalization group	Janssen & Stenull (2011)[49]
5	9/17=0.529	5/9=0.556	5/17 = 0.294	0.0091	26%	Flory theory	This work
5	–	–	**0.2849 ± 0.0002**	–	–	Renormalization group	Janssen & Stenull (2011)[49]
6	1/2=0.5	1/2=0.5	1/4 = 0.25	0	0%	Flory theory	This work
6	–	–	**0.25**	–	–	Renormalization group	Janssen & Stenull (2011)[49]

Table 4

Analytical and simulation results for critical exponents ρ, ν_{path} and ν of annealed lattice trees in melts for different spatial dimensionalities d. $\frac{\delta\nu}{\delta\nu_{\text{ideal}}}$ is defined as in Table 1. Currently available exact values or best estimates (in boldface) are reported as symbols in Fig. 3, where predictions of Flory theory are shown as lines. To our knowledge, analytical or simulation data for quenched branched polymers in melts are currently missing.

Annealed branching polymers in melts

d	ρ	ν_{path}	ν	$\delta\nu$	$\frac{\delta\nu}{\delta\nu_{\text{ideal}}}$	Technique	Reference
2	2/3=0.667	3/4=0.75	1/2 = 0.5	0.02	9%	Flory theory	Grosberg (2014)[18]
2	**0.613 ±0.007**	**0.780 ±0.005**	**0.48 ±0.02**	–	–	Monte Carlo	Rosa & Everaers (2016)[63]
3	5/9=0.556	3/5=0.6	1/3 = 0.333	0.013	19%	Flory theory	Grosberg (2014)[18]
3	**0.52 ±0.05**	**0.593 ±0.007**	**0.32 ±0.02**	–	–	Monte Carlo	Rosa & Everaers (2016)[63]